JACS
JOURNAL OF THE AMERICAN CHEMICAL SOCIETY
Article
pubs.acs.org/JACS

Efficient Uranium Capture by Polysulfide/Layered Double Hydroxide Composites

Shulan Ma,[†,‡] Lu Huang,[†] Lijiao Ma,[†] Yurina Shim,[‡] Saiful M. Islam,[‡] Pengli Wang,[‡] Li-Dong Zhao,[‡,§] Shichao Wang,[‡] Genban Sun,[†] Xiaojing Yang,[†] and Mercouri G. Kanatzidis*[,‡]

[†]Beijing Key Laboratory of Energy Conversion and Storage Materials, College of Chemistry, Beijing Normal University, Beijing 100875, China

[‡]Department of Chemistry, Northwestern University, 2145 Sheridan Road, Evanston, Illinois 60208, United States

[§]School of Materials Science and Engineering, Beihang University, Beijing, 100191, China

ABSTRACT: There is a need to develop highly selective and efficient materials for capturing uranium (normally as UO_2^{2+}) from nuclear waste and from seawater. We demonstrate the promising adsorption performance of S_x-LDH composites (LDH is Mg/Al layered double hydroxide, $[S_x]^{2-}$ is polysulfide with x = 2, 4) for uranyl ions from a variety of aqueous solutions including seawater. We report high removal capacities (q_m = 330 mg/g), large K_d^U values (10^4–10^6 mL/g at 1–300 ppm U concentration), and high % removals (>95% at 1–100 ppm, or ~80% for ppb level seawater) for UO_2^{2+} species. The S_x-LDHs are exceptionally efficient for selectively and rapidly capturing UO_2^{2+} both at high (ppm) and trace (ppb) quantities from the U-containing water including seawater. The maximum adsorption coeffcient value K_d^U of 3.4 × 10^6 mL/g (using a V/m ratio of 1000 mL/g) observed is among the highest reported for U adsorbents. In the presence of very high concentrations of competitive ions such as Ca^{2+}/Na^+, S_x-LDH exhibits superior selectivity for UO_2^{2+}, over previously reported sorbents. Under low U concentrations, $(S_4)^{2-}$ coordinates to UO_2^{2+} forming anionic complexes retaining in the LDH gallery. At high U concentrations, $(S_4)^{2-}$ binds to UO_2^{2+} to generate neutral UO_2S_4 salts outside the gallery, with NO_3^- entering the interlayer to form NO_3-LDH. In the presence of high Cl^- concentration, Cl^- preferentially replaces $[S_4]^{2-}$ and intercalates into LDH. Detailed comparison of U removal efficiency of S_x-LDH with various known sorbents is reported. The excellent uranium adsorption ability along with the environmentally safe, low-cost constituents points to the high potential of S_x-LDH materials for selective uranium capture.

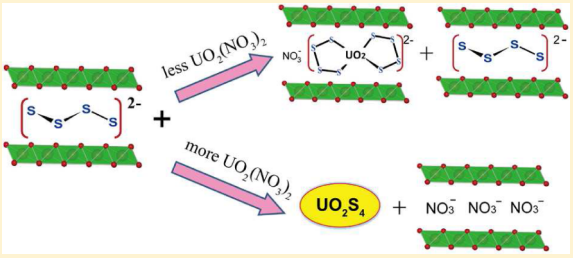

INTRODUCTION

Uranium is the main source of nuclear energy[1] used in nuclear reactors and is a dominant component in the nuclear waste they generate.[2] Interestingly, uranium is also naturally present in seawater where its concentration is low (approximately 3–9 ug/L),[3,4] while the total amount in the oceans is about 4.5 billion tons.[3] It has been suggested that this is a potential huge resource that could supply uranium for nuclear energy for several thousand years, and as a result there is a strong motivation to develop sorbents that selectively pull uranium from nuclear waste as well as seawater.

Many kinds of methods have been employed for uranium removal from nuclear waste including liquid–liquid extraction,[5,6] ion-exchange/absorption,[7−9] adsorption,[10−12] and chemical/biochemical reductive precipitation.[13−16] Specifically, adsorption is a convenient method, which is generally employed by chemically modified adsorbents such as modified activated carbon,[17] activated carbon-silica aerogel composite materials,[18] barium titanate,[19] gallocyanine grafted hydro-gel,[20] ion-imprinted polymers,[21] and polyphenolic compounds.[22−27] Among these, the organics show relatively low thermal stability which could be a disadvantage for the practical use. On the contrary, inorganic materials especially those with exchangeable ions, such as clays and zeolites, generally exhibit higher chemical and thermal stability. For this reason, many inorganic adsorbents have been investigated for uranium removal (e.g., UO_2^{2+}).[28,29] Slow ion-exchange kinetics, however, between the inorganic exchangers and the large hydrated $[UO_2(H_2O)_x]^{2+}$ ion as well as competition from other ions often limit their application.[30] In addition, mineral sulfides such as FeS_2 have been tested as uranium scavengers,[31,32] but their nonporous structure makes them adsorb metal ions only on the surface, which results in limited adsorption capacity.[33,34] Therefore, new materials are of interest as current methods for uranium removal have the above-mentioned disadvantages.

In aqueous solutions, uranium exists mainly as a hexavalent state in the most stable form of uranyl ion (UO_2^{2+}), which is regarded as a hard cation in the Lewis acid sense. However, our previous studies demonstrated that UO_2^{2+} can still easily form covalent bonds with soft S^{2-} groups.[35,36] In the layered sulfides specifically the KMS-1 ($K_{2x}Mn_xSn_{3-x}S_6$, x = 0.5–0.95), we have observed that strong $UO_2^{2+}\cdots S^{2-}$ bonding interactions contribute to the uranium removal.[37] These results suggest

Received: January 22, 2015
Published: February 25, 2015

DOI: 10.1021/jacs.5b00762
J. Am. Chem. Soc. 2015, 137, 3670–3677

that the $[UO_2]^{2+}$ ion is a much softer Lewis acid center than previously thought. Taking this as a new insight, it suggests alternative strategies on how to approach the capture problem. Such strategies should point to utilizing $UO_2^{2+}\cdots S^{2-}$ bonding interactions as a possible mechanism for selective binding. We previously developed aerogels made with metal sulfides, termed *chalcogels*, and these materials have shown high efficiency in capturing radionuclides including uranium.[38]

Here we show that polysulfide intercalated layered double hydroxides (LDHs) are good uranium removal materials consistent with the hypothesis that $UO_2^{2+}\cdots S^{2-}$ bonding interactions can selectively remove this ion. The LDH compounds are a well-known, extensively studied class of layered anionic clays and exhibit excellent intercalation and anion-exchange properties.[39] These properties allow the LDH materials to be used in various applications such as catalysts,[40,41] two-dimensional nanoreactors,[42,43] adsorbents, and scavengers.[44,45] Recently, we described the introduction of polysulfide anions $[S_x]^{2-}$ into the gallery space of LDH.[46−48] We expect the combination of polysulfide anions with the LDH layers to be a powerful advantage producing materials capable of possessing soft Lewis basic binding sites, to be used for uranium capture efficiency studies. We show that the polysulfide/LDH composites (S_x-LDH, x = 2, 4), are exceptionally capable of selective and fast sequestration of uranium in the form of UO_2^{2+} in a wide range of uranium concentrations (5 ppb to 5000 ppm), even in the presence of various kinds of competitive ions. Moreover, we observe efficient U removal in potable water and seawater, making the S_x-LDH one of the most powerful uranium (U) adsorbents reported with high potential in future applications.

EXPERIMENTAL SECTION

Materials. The K_2S_4 precursor was synthesized by the reaction of elemental K and S in liquid ammonia as described elsewhere.[49] The MgAl-NO_3-LDH was prepared through NO_3^-/CO_3^{2-} ion-exchange using MgAl-CO_3-LDH as precursor.[50−53] The $[S_x]^{2-}$ (x= 2, 4) anions in K_2S_x were exchanged with NO_3^- of the NO_3-LDH to get S_x-LDH, as we previously reported.[46]

Uranium Uptake Experiments. The uranium uptake from aqueous solutions of various concentrations and seawater was carried out by the batch method. The solid sorbents of S_4-LDH and S_2-LDH were immerged with the solutions with intermittent shaking for 24 h and 3 days. After mixing the solid sorbents with the solutions for a certain time (10−30 min), a centrifugation was performed, and the concentrations of metal ions in the supernatant solution were determined using inductively coupled plasma-atomic emission spectroscopy (ICP-AES) and for extra low ion concentration (≤ppb) inductively coupled plasma-mass spectroscopy (ICP-MS). The adsorptive capacity was evaluated from the difference of metal concentrations in mother and supernatant solutions.

The distribution coefficient K_d is defined by the equation:

$$K_d = (V[(C_0 - C_f)/C_f])/m$$

where C_0 and C_f are, respectively, the initial and local concentration of M^{n+} (ppm, μg/mL) after the contact, V is the volume (mL) of the testing solution, and m is the amount of the solid sorbent (g) used in the experiment.[54] In our above experiments, V/m ratios of 100−1000 mL/g were used. The capture efficiency, referred as removal (%), was calculated with the equation:

$$\%\text{removal} = 100 \times (C_0 - C_f)/C_0$$

The removal capacity (q_m) is calculated using the equation $10^{-3} \times (C_0 - C_f)\cdot V/m$.

The UO_2^{2+} uptake from solutions of various concentrations (10−600 ppm) was studied using S_2-LDH and S_4-LDH by the batch method at V/m = 1000 mL/g, room temperature, and 24 h contact. The competitive capture experiments of UO_2^{2+} (U: 1−4 ppm) with excess Ca^{2+} ($CaCl_2$/U molar ratios: 1×10^3−6×10^4) or Na^+ (Na/U molar ratios: 2×10^4−4×10^4) using S_4-LDH were carried out at V/m ratio of 1000 mL/g, room temperature, and 24 h contact.

Adsorption studies with tap water intentionally contaminated with UO_2^{2+}, natural seawater (from the Bohai Bay region located near Tianjin City of China), and contaminated seawater (created by adding ∼30 ppb UO_2^{2+} to the seawater) were also performed. For each experiment, a total of 0.15 g of S_4-LDH was weighted into a 50 mL centrifugal tube. Then a 15 mL of water solution was added to each tube, and the mixture was kept under stirring for 24 h (V/m ratio = 100 mL/g).

Kinetic Studies. UO_2^{2+} adsorption experiments under various adsorption times (10−180 min) were performed. For each experiment, 0.25 g of solid sample was weighted into a 50 mL centrifugal tube, and a 25 mL aqueous solution containing UO_2^{2+} (∼7 ppb) was added to each tube (V/m = 100 mL/g). The suspensions from the various operations were centrifuged, and the resulting supernatant solutions were analyzed by ICP-MS to get their uranium contents.

Reaction of S_4-LDH with Excess UO_2^{2+}. A reaction of S_4-LDH with excess UO_2^{2+} was carried out as follows: 0.11 g S_4-LDH (1.2 mmol, which contains 0.15 mmol $(S_4)^{2-}$) was added to a solution of 0.36 g $UO_2(NO_3)_2\cdot 5H_2O$ (0.72 mmol) in ultrapure water (20 mL), where the U concentration is ∼8500 ppm and V/m ratio is ∼180. After 24 h reaction, the darker yellow solid was isolated by centrifugation, washed with enough water (∼100 mL), and acetone (∼20 mL), respectively, followed by drying in air. CHN and ICP-AES analyses were used to determine the composition of the product. Powder X-ray diffraction (XRD) were performed for structural information; morphology and elemental compositions were analyzed by scanning electron microscopy (SEM); and energy dispersive X-ray spectroscopy (EDS), respectively.

Control Experiment: Reaction of S_x^{2-} and $(UO_2)^{2+}$. 0.15 g K_2S_4 (0.75 mmol) was first mixed with 0.30 g $UO_2(NO_3)_2$ (0.75 mmol) into a little vial in a nitrogen filled glovebox. Then the vial was taken out from the glovebox, and distilled water (10−20 mL) was added. After about 6 h reaction, the obtained yellow-brown solid (UO_2S_4) was isolated by filtration and washed with enough water (∼50 mL) and acetone (∼20 mL).

Characterization Techniques. The XRD patterns were collected using a PANalytical X'pert Pro MPD diffractometer with Cu−Kα radiation at room temperature, with step size of 0.0167°, scan time of 10 s per step, and 2θ ranging from 4.5 to 70°. The generator setting is 40 kV and 40 mA. Fourier transformed infrared (FT-IR) spectra of the samples were recorded on a Nicolet-380 Fourier-Transform infrared spectrometer using the KBr pellet method. SEM and EDS measurements and elemental distribution mappings were carried out using a Hitachi S-4800 microscope. X-ray photoelectron spectroscopy (XPS) was recorded on an ESCALAB 250Xi spectrometer (Thermo Fisher). Fitting of the peaks was performed by Avantage software.

The metal ion concentrations in solution before and after adsorption were measured using ICP-AES (Jarrel-ASH, ICAP-9000) and ICP-MS (NexION 300X) for extra low concentrations. For determining the composition of some solid samples, ICP-AES (a ∼0.1 M HNO_3 solution was used to dissolve the solids beforehand for doing the ICP) and CHN analyses using an Elementar Vario EL elemental analyzer were conducted.

RESULTS AND DISCUSSION

Removal of Uranyl Ion from Solution. To evaluate the ability of S_x-LDH to adsorb UO_2^{2+}, we performed batch reaction studies. As seen in Tables 1 and 2, for S_4-LDH and S_2-LDH, the uranium uptake increased with increasing uranium concentration. The maximum removal capacities (q_m) (for definition, see Experimental Section) of both materials were calculated to be ∼330 mg/g, being comparable to those of the best reported uranium adsorbents (307−380 mg/g).[26,27,37] It

DOI: 10.1021/jacs.5b00762
J. Am. Chem. Soc. 2015, 137, 3670−3677

Table 1. UO_2^{2+} Adsorption Efficiency of S_4-LDH[a]

C_0[b] (ppm)	pH	C_f[c] 24 h (ppm)	pH	U capacity, q_m (mg/g)	removal (%)	K_d (mL/g)
22.1	6.2	0.006	7.4	22.1	99.97	3.4×10^6
48.7	5.8	0.1	6.8	48.6	99.75	3.9×10^5
76.4	5.3	2.6	6.5	73.7	96.52	2.8×10^4
121.4	4.8	9.4	6.1	112.0	92.25	1.2×10^4
242.4	4.6	100.7	5.7	141.7	58.44	1.4×10^4
301.5	4.4	141.3	5.6	160.1	53.12	1.1×10^4
345.2	4.2	161.5	5.5	183.7	53.22	1.1×10^4
547.9	3.9	343.1	4.9	204.8	37.38	6.0×10^2
1478.2	3.5	1146.5	4.0	331.7	22.44	2.9×10^2

[a] m: 0.030 g, V: 30 mL, V/m = 1000 mL/g. Contact time: ~24 h. [b] C_0, initial uranium concentration. [c] C_f, final uranium concentration after 24 h adsorption.

Table 2. UO_2^{2+} Adsorption Efficiency of S_2-LDH[a]

C_0 (ppm)	pH	C_f, 3d (ppm)	pH	U capacity, q_m (mg/g)	removal (%)	K_d (mL/g)
48.7	5.8	0.06	6.9	48.64	99.9	8.4×10^5
144.8	5.1	4.7	6.4	140.08	96.8	3.0×10^4
242.4	4.6	94.7	5.8	147.77	61.0	1.6×10^3
345.2	4.2	164.4	5.4	180.85	52.4	1.1×10^3
547.9	3.9	365.4	4.7	182.48	33.3	5.0×10^2
825.5	3.7	646.6	4.3	179.00	21.7	2.8×10^2
1478.2	3.5	1148.4	3.9	329.72	22.31	2.9×10^2

[a] m: 0.030 g, V: 30 mL, V/m = 1000 mL/g. Contact time: ~3 d.

can be seen in Table 1, for S_4-LDH, the U removal reaches high values of 96.52–99.97% over a wide range of U initial concentration (20–100 ppm). For S_2-LDH, the U removal is over 96% in the concentration of 40–150 ppm (Table 2).

The affinity of the materials for UO_2^{2+} can be expressed in terms of the distribution coefficient K_d^U (for definition, see Experimental Section and ref 9) for specific experimental conditions. Generally, a material with a K_d value >10^4 mL/g is considered to be an excellent adsorbent.[54,55] In the case of S_4-LDH, at an uranium concentration range of 20–350 ppm, the K_d values ranged from 1.1×10^4 to 3.4×10^6 mL/g (Table 1). The K_d value of 3.4×10^6 mL/g appears to be among the highest reported for U adsorbents (Table 3).[7,37] For S_2-LDH, the K_d values also reached up to 8.4×10^5 mL/g (Table 2).

The uranium capture by S_x-LDH was detected by EDS analyses, elemental distribution mapping, and XPS spectroscopy. EDS of the S_4-LDH sample after adsorption of UO_2^{2+} using an initial concentration of 345 ppm (Figure 1b) showed a S/U

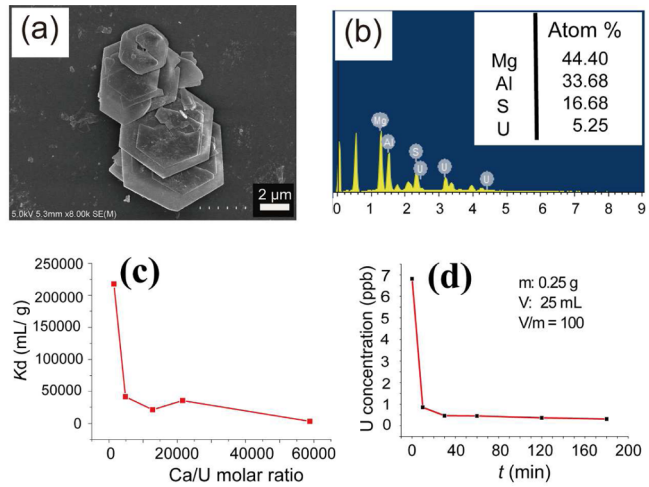

Figure 1. (a) SEM image and (b) EDS of the resulting product after S_4-LDH adsorbed UO_2^{2+} (345 ppm), (c) K_d^U with Ca/U molar ratios of 1500–60,000, (d) kinetics of U adsorption by S_4-LDH at 7 ppb initial U concentration (V/m = 100 mL/g).

molar ratio of 3–4, which coincides with the bonding of one $[S_4]^{2-}$ group (containing four S sites) to one UO_2^{2+}. Elemental distribution mapping of the sample (Figure 2(a-4)) showed the

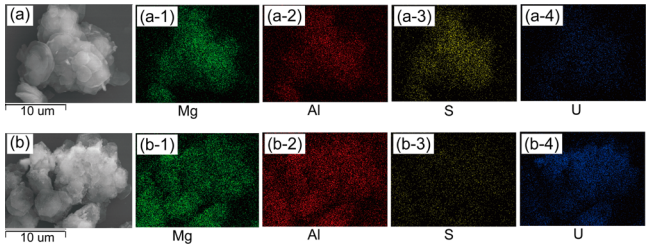

Figure 2. SEM images of (a) the sample after S_4-LDH adsorbed 345 ppm U and (b) the "reacted sample" S_4-LDH-U (a-1) to (a-4) and (b-1) to (b-4) show corresponding elemental distribution maps of Mg, Al, S, and U for (a) and (b).

Table 3. U Removal Efficiency of Various Adsorbents in This Work and References

	U capacity, q_m (mg/g)	U removal (%)	K_d^U (mL/g)	ref
S_x-LDH	330	99.97	1.1×10^4–3.4×10^6	this work
KMS-1[a]	380	99.9	1.1×10^4–1.8×10^5	37
chalcogen-based aerogels[b]	–	68.1–99.4	$(3.1–9.4) \times 10^4$	38
U-pass[c]	148	>97	–	21
HSDC[d]	373	–	–	26
HTC-btg[e]	307	–	–	27
SAMMS[f]	–	–	2.8×10^3–1.6×10^5	9
Cs-birnessite	–	~100	1.6×10^6	7
Li-birnessite	–	99.9	1.8×10^5	7
Na-birnessite	–	99.6	4.9×10^4	7
K-birnessite	–	99.8	8.8×10^4	7

[a] Layered sulfide ion exchanger $K_2MnSn_2S_6$ (KMS-1). [b] Chalcogels are $Co_{0.7}Bi_{0.3}MoS_4$, $Co_{0.7}Cr_{0.3}MoS_4$, $Co_{0.5}Ni_{0.5}MoS_4$, $PtGe_2S_5$, and Sn_2S_3. [c] Uranyl ion-imprinted microspheres. [d] HSDC: polyphenolic-hydroxyl functionalized material. [e] HTC-btg: a catechol-like ligand–functionalized hydrothermal carbon sorbent. [f] SAMMS: self-assembled monolayers on mesoporous supports.

DOI: 10.1021/jacs.5b00762
J. Am. Chem. Soc. 2015, 137, 3670–3677

presence of significant amount of captured uranium and its homogeneous distribution in the sample. XPS spectra (Figure 3b) exhibited strong U 4f peaks, which further confirms the U presence, being in good agreement with the EDS results.

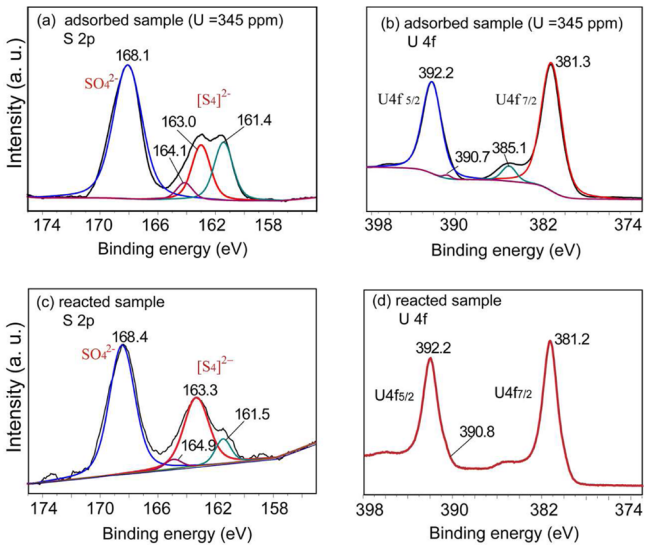

Figure 3. XPS spectroscopy with the deconvolution of corresponding XPS peaks: S 2p and U 4f spectra of (a, b) U adsorbed sample (345 ppm) and (c, d) "reacted sample" S_4-LDH-U.

XRD patterns of the samples after adsorption using various uranium concentrations (Figure 4A) showed significant change.

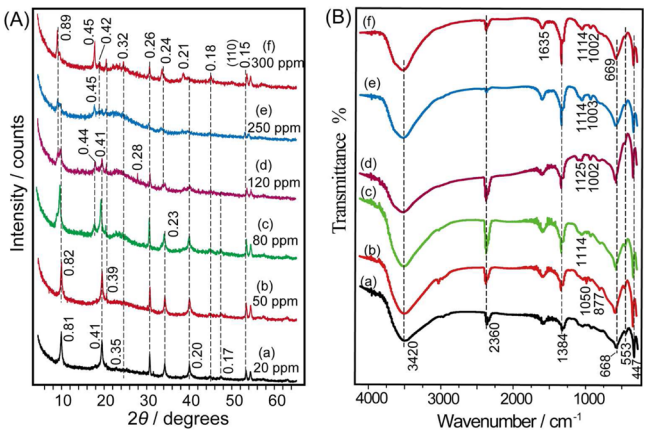

Figure 4. (A) XRD patterns and (B) IR spectra of the resulting samples after S_4-LDH adsorbed UO_2^{2+} at (a) 20, (b) 50, (c) 80, (d) 120, (e) 250, and (f) 300 ppm. In XRD, the *d*-values are given in nanometers.

At low U concentration (<50 ppm), the basal spacings (d_{basal}) of 0.81/0.82 nm observed are the same as the pristine S_x-LDH material before adsorption. At the concentration of 50−120 ppm, an additional peak appeared at 0.89 nm, resulting from the intercalation of NO_3^- into LDH, and increased in intensity with the increasing U concentration. At concentrations ≥120 ppm, the d_{basal} spacing at 0.89 nm is dominant over the 0.82 nm spacing. Additionally, the peak at d = 0.15 nm corresponding to the (110) plane signifies that the structure of the LDH sheet does not change during the adsorption process.

The U adsorption and stability of S_x-LDH were also confirmed by the IR spectra (Figure 4B). An obvious band at 1384 cm^{-1} occurs for all solid samples after U adsorption, implying the presence of NO_3^- anions which accompanied the UO_2^{2+} cations for charge balance. The increased intensity of the 1384 cm^{-1} band with increasing U concentration reflects the increasingly adsorbed amount of uranium. The unchanged ν(M−O) vibrations at 668/669 cm^{-1} and δ(O−M−O) modes at 447 cm^{-1}[56,57] indicate the stability of LDH layer undergoing the adsorption process. The retained hexagonal prismatic morphology of the S_x-LDH after the uranium adsorption is evident in the SEM images of S_4-LDH as shown in Figure 1a.

The XPS spectra could be fitted by a single contribution of U^{6+} state with binding energy values at 392.2 eV (U $4f_{5/2}$) and 381.3 eV (U $4f_{7/2}$),[37,58] indicating the absence of redox activity during the interaction with polysulfide groups.[32,59] The binding energies ranging from 160.0 to 163.6 eV represent the $[S_n]^{2-}$ groups.[60,61] Additionally, the small peaks at ∼164.1[62] and ∼168.1 eV are suggestive of S_n^0 and SO_4^{2-} (generally appears at 168−171 eV)[62] which come from the partial oxidation of $[S_4]^{2-}$, upon exposure to O_2 in water. The polysulfide $[S_4]^{2-}$ is formally composed of S^{2-} + $3S^0$, in which the S^{2-} ion is not stable in air and in certain conditions can be oxidized by the O_2 coming from air or water to form SO_4^{2-}.

Effect of Competitive Cations Ca^{2+} and Na^+ on UO_2^{2+} Adsorption. As Ca^{2+} ions exist in relatively high concentrations in wastewater, it can strongly compete for the selectivity of sorbents consequently we investigated the effect of $CaCl_2$ salt on the UO_2^{2+}-sorption. As shown in Tables 1 and 2, the adsorption efficiencies of S_4-LDH and S_2-LDH are similar, but that of S_4-LDH is slightly better. For this reason, we conducted our subsequent investigations using only S_4-LDH. From Table 4 and Figure 1c, S_4-LDH had a remarkably higher selectivity for UO_2^{2+} over Ca^{2+}. Large removal capacities (95−99%) and K_d^U values (2.1 × 10^4−2.1 × 10^5 mL/g) were still obtained at high $CaCl_2$/U molar ratios of 1.5 × 10^3−2.1 × 10^4. It is noted that even with a tremendous excess of $CaCl_2$ ($CaCl_2$/U molar ratio ≈6 × 10^4), the S_4-LDH still gave significantly higher UO_2^{2+} removal efficiency (76%) and high K_d^U value of 3.1 × 10^3 mL/g, being superior to the best uranium adsorbents reported.[37] All these data demonstrate a high selectivity of S_4-LDH for UO_2^{2+} over large excess of Ca^{2+}. The strong affinity of S_4-LDH for UO_2^{2+} in the presence of high Ca^{2+} concentrations arises from the stronger soft−soft acid-based $UO_2^{2+}\cdots S^{2-}$ bonding interactions compared to hard−soft $Ca^{2+}\cdots S^{2-}$ interactions.

The structure of S_4-LDH is retained after the adsorption process with the mixed Ca/U solutions as evidenced by the XRD patterns (see Figure 5). At a Ca/U molar ratio of 1500, the d_{basal} spacing was at 0.80 nm, the same as the starting material, while at high Ca/U molar ratios (>5000), additional d_{basal} spacings at 0.78/0.77 nm appeared, indicating the intercalation of Cl^- into the LDH gallery to form Cl-LDH as a separate and dominant phase.

We also tested the performance of S_4-LDH in the presence of a large excess of Na^+, since very high concentrations of sodium are present in seawater and in nuclear wastewater.[37] An exceptional ability of S_4-LDH to adsorb UO_2^{2+} (≥97% U removal capacity) in the presence of a tremendous excess of NaCl (40,000-fold) or $NaNO_3$ (20,000-fold) was observed (see Table 4), and the K_d^U values were higher than 10^4 mL/g, even reaching up to 10^5 mL/g. These values reveal high selectivity of S_4-LDH for UO_2^{2+} against Na^+.

The intercalation of Cl^- anions was also observed after S_4-LDH adsorbed uranium in the presence of large amount of

DOI: 10.1021/jacs.5b00762
J. Am. Chem. Soc. 2015, 137, 3670−3677

Table 4. Adsorption of S_4-LDH for UO_2^{2+} with Competitive Ions of Ca^{2+} or Na^{+a}

		pH		Ca		U			
	Ca/U ratio	initial	final	C_0 (ppm)	C_f, 24 h (ppm)	C_0 (ppm)	C_f, 24 h (ppm)	U removal (%)	K_d^U (mL/g)
$CaCl_2$ + U	1483	6.13	6.27	928	902	3.72	0.017	99.5	2.1×10^5
	4856	6.20	6.35	1940	1928	2.38	0.056	97.6	4.1×10^4
	12797	6.26	6.40	3864	3696	1.80	0.081	95.5	2.1×10^4
	21574	6.28	6.41	6748	6608	1.86	0.051	97.3	3.5×10^4
	58828	6.31	6.43	12779	12137	1.29	0.314	75.7	3.1×10^3
		pH		Na		U			
	Na/U ratio	initial	final	C_0 (ppm)	C_f, 24 h (ppm)	C_0 (ppm)	C_f, 24 h (ppm)	U removal (%)	K_d^U (mL/g)
NaCl + U	40,000	6.54	6.57	10734 (0.47 M)	10682	2.73	0.081	97.0	3.3×10^4
$NaNO_3$ + U	20,000	6.65	6.70	4428 (0.20 M)	4401	2.36	0.02	99.2	1.2×10^5

[a] m: 0.030 g, V: 30 mL. V/m = 1000 mL/g. For $CaCl_2$ + U, the contact time is ~24 h; for NaCl + U and $NaNO_3$ + U, contact time is 3 d.

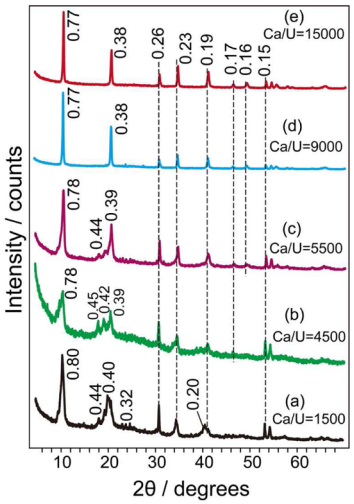

Figure 5. XRD patterns of the samples after S_4-LDH adsorbed (a–e) Ca/U mixed ions at different Ca/U molar ratios. The d-values are given in nanometers.

NaCl. The XRD patterns (Figure 6a) revealed that following the binding of UO_2^{2+}, Cl^- anions were intercalated into the

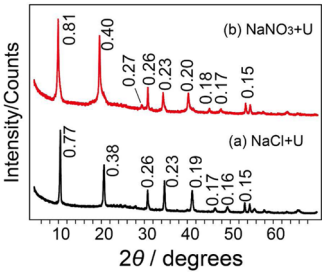

Figure 6. XRD patterns of the samples after S_4-LDH adsorbed (a) NaCl + U and (b) $NaNO_3$ + U. The d-values are given in nanometers.

LDH gallery to form Cl-LDH with the d_{basal} of 0.77 nm, as observed in the aforementioned $CaCl_2$ + U system. Therefore, in $CaCl_2$ + U or NaCl + U cases with much higher Cl^- concentration, due to the strong affinity of Cl^- to LDH layer (trend is $CO_3^{2-} > SO_4^{2-} > OH^- > F^- > Cl^- > Br^- > NO_3^-$),[50] Cl^- ions preferentially displace the $(S_4)^{2-}$ and enter the interlayer, meanwhile, the $(S_4)^{2-}$ bonds with UO_2^{2+} to form UO_2S_4 outside the gallery. It is noteworthy that, in the case of $NaNO_3$ + U, though the $NaNO_3$ concentration is also very high, no d_{basal} of 0.89 nm for NO_3-LDH was found in the XRD pattern (Figure 6b). This is attributed to the lower affinity of NO_3^- for the LDH layer.

U Capture from Wastewater and Seawater and Adsorption Kinetics. Because of the excellent uranium removal ability of S_x-LDH presented above, we examined the applicability of S_4-LDH in the remediation of natural water samples and contaminated water with low concentration of UO_2^{2+} ([U] ~ 5–30 ppb) (Table 5, V/m = 100 mL/g). In order to test the performance of S_4-LDH for decontaminating tap water, in which other ions including Ca^{2+} (73.8 ppm), K^+ (4.38 ppm), Mg^{2+} (23.6 ppm), and Na^+ (21.2 ppm) are present, we spiked it with ~20 ppb U. At this low U level in tap water, the % removal was >75%. Meanwhile, at an extremely low concentration of naturally occurring uranium (~9 ppb) in seawater (collected from Bohai bay region located by Tianjin City of China), which contains extremely high concentration of other ions such as Na^+ (9279 ppm), Mg^{2+} (1063 ppm), Ca^{2+}

Table 5. Uranium Adsorption of S_4-LDH Towards Contaminated Potable Water and Contaminated and Original Seawater[a]

		C_0^U (ppm)	C_f^U, 24 h (ppm)	% removal (U)
contaminated potable water	Ca^{2+} (73.8 ppm) K^+ (4.38 ppm) Mg^{2+} (23.6 ppm) Na^+ (21.2 ppm)	0.020	0.005	75.0
pH		7.10 → 8.10		
contaminated seawater	Ca^{2+} (359 ppm) K^+ (374 ppm) Mg^{2+} (1020 ppm) Na^+ (8981 ppm)	0.030	0.007	76.7
pH		8.30 → 8.31		
original seawater	Ca^{2+} (375 ppm), K^+ (396 ppm) Mg^{2+} (1063 ppm) Na^+ (9279 ppm)	0.009	0.002	77.8
pH		8.55 → 8.29		

[a] m: 0.15 g, V: 15 mL, V/m = 100 mL/g. Contact time, 24 h.

DOI: 10.1021/jacs.5b00762
J. Am. Chem. Soc. 2015, 137, 3670–3677

(375 ppm), and K^+ (396 ppm), the final U concentration was decreased to ≤2 ppb, achieving a 78% removal. Further experiments were performed by adding 30 ppb U to this kind seawater, and the % removal of U was similar at 77%, with a final U concentration ≤7 ppb. These results suggest that S_4-LDH is a promising uranium adsorbent even for seawater where the ratio of other ions (Ca^{2+}, K^+, Mg^{2+}, and Na^+) to uranium is overwhelming. The ability of S_4-LDH to adsorb uranium from seawater is comparable with the best reported materials[37,63] and underscores the potential of S_4-LDH for sequestering U from the sea.[64] Once the materials are saturated with uranium, we anticipate that they can be used to recover the metal using post processing techniques. The high concentration of uranium in the solid and the low cost of the LDH should allow the recovery without the need for regenerating the material. The constituent of the LDH material however could be captured and recycled.

The kinetics of adsorption process by S_4-LDH was investigated with an added U concentration of 7 ppb (Table 6) in the distilled water. The adsorption by S_4-LDH was found

Table 6. Kinetics Data of UO_2^{2+} Adsorption Using S_4-LDH (an Aqueous Solution with an Initial U Concentration of ∼7 ppb)[a]

C_0 (ppb)	t (min)	C_f (ppb)	removal (%)	K_d (mL/g)
6.82	10	0.85	87.6	7.0×10^2
	30	0.46	93.3	1.4×10^3
	60	0.45	93.5	1.4×10^3
	120	0.36	94.8	1.8×10^3
	180	0.31	95.5	2.1×10^3

[a] m: 0.25 g, V: 25 mL, V/m = 100 mL/g.

to be very fast (Figure 1d), and the final U concentration became ≤1 ppb within 10 min of treatment toward the solution (V/m = 100 mL/g). Namely, the adsorption reached 95% removal and K_d of 2.1×10^3 mL/g in 180 min.

Reaction of S_4-LDH with Excess $UO_2(NO_3)_2$. To understand the reaction between UO_2^{2+} and $[S_4]^{2-}$, an $UO_2^{2+}/[S_4]^{2-}$ molar ratio of 5 (excess $UO_2(NO_3)_2$) was used to ensure the complete reaction of UO_2^{2+} with $[S_4]^{2-}$. Here a much larger U concentration of ∼8500 ppm was used. In order to distinguish the samples in this experiment and those obtained from the adsorption, we refer to the former as "reacted sample" and the latter as "adsorbed sample". The XRD patterns of the "reacted sample" (Figure 7a) showed a d_{basal} spacing of 0.88 nm, which is close to the d_{basal} (0.87 nm) for SO_4-LDH (Figure 7a-1) and that (0.89 nm) for NO_3-LDH (Figure 7a-3). Also, the S 2p binding energy at 168.4 eV, attributed to SO_4^{2-},[62] was observed in the XPS spectra (Figure 3c). The strong NO_3^- adsorption (1384 cm^{-1} band) in the IR spectra (Figure 7b) and very weak SO_4^{2-} adsorption (expected at 1108 cm^{-1} as in Figure 7b-1) suggest that NO_3^- intercalated LDH is formed and the amount of SO_4^{2-} is negligible.

In the "reacted sample", the UO_2^{2+} binding with $[S_4]^{2-}$ forms neutral salts outside the gallery and LDH-NO_3. The new strong IR band at ∼913 cm^{-1} in the "reacted sample" (Figure 7b) is assigned to the antisymmetric vibration of $[O{=}U^{6+}{=}O]^{2+}$.[21,27,37,65] This peak has a significant red-shift compared to the corresponding peak of aqueous UO_2^{2+} (∼963 cm^{-1}),[66] indicating the chemical bonding of UO_2^{2+} with the $[S_4]^{2-}$ group.[21,37,65] Strong and sharp U 4f peaks were also observed in the "reacted sample" (Figure 3d), confirming the presence of U.

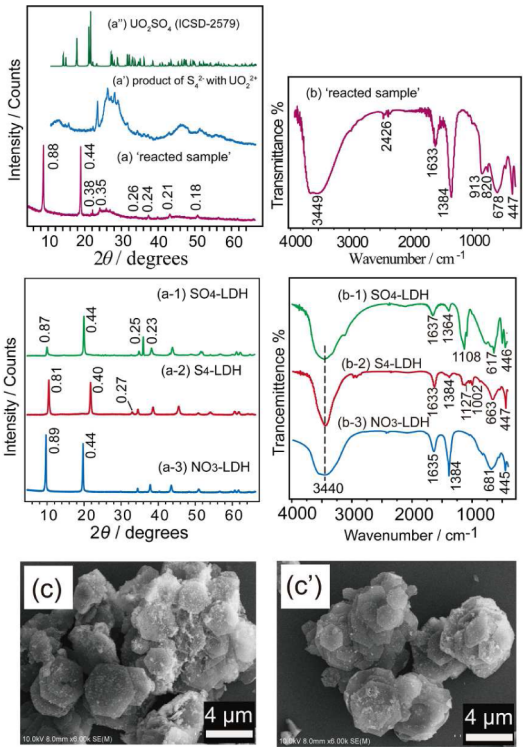

Figure 7. XRD patterns of "reacted sample" S_4-LDH-U (a), product of S_4^{2-} with UO_2^{2+} (a′), standard pattern of UO_2SO_4 (a″), control samples SO_4-LDH (a-1), S_4-LDH (a-2), and NO_3-LDH (a-3), IR spectra of "reacted sample" S_4-LDH-U (b) and control samples SO_4-LDH (b-1), S_4-LDH (b-2), and NO_3-LDH (b-3), and SEM images of the "reacted sample" S_4-LDH-U (c, c′).

Specifically, the single contribution of the U^{6+} oxidation state, indicated by the binding energies of 392.2 eV (U $4f_{5/2}$) and 381.2 eV (U $4f_{7/2}$),[37,58] suggests no uranium reduction is occurring. Elemental distribution maps revealed an uniform distribution of U element in the samples (Figure 2b-4).

CHN and ICP analyses (Table 7) suggest the chemical formula of the starting material S_4-LDH is $Mg_{0.66}Al_{0.34}(OH)_2(S_4)_{0.13}(NO_3)_{0.01}(CO_3)_{0.04}{\cdot}0.8H_2O$, and the "reacted sample" (named as S_4−LDH-U) is a mixture of NO_3-LDH + $(UO_2)_{0.22}(S_4)_{0.10}(SO_4)_{0.12}$. The experimentally deter-

Table 7. Chemical Compositions of S_4-LDH and "Reacted Sample" S_4-LDH-U

	wt %, found (calcd)[a]					
	Mg	Al	U	C	H	N
S_4-LDH[b]	16.72 (17.02)	10.26 (9.90)	–	0.49 (0.52)	3.84 (3.87)	0.11 (0.15)
S_4-LDH-U[c]	10.29 (10.47)	5.89 (6.00)	34.43 (34.11)	0.30 (0.23)	2.31 (2.35)	2.41 (2.45)

[a] C, H, and N contents were determined by CHN analyses, and the U amount was obtained by ICP. [b] Chemical formula of S_4-LDH is $Mg_{0.66}Al_{0.34}(OH)_2(S_4)_{0.13}(NO_3)_{0.01}(CO_3)_{0.04}{\cdot}0.8H_2O$. [c] Formula of the reacted sample S_4-LDH-U is $Mg_{0.67}Al_{0.33}(OH)_2(NO_3)_{0.27}(CO_3)_{0.03}{\cdot}1.8H_2O + (UO_2)_{0.22}(S_4)_{0.10}(SO_4)_{0.12}$. The latter part is first written as $(UO_2)_{0.22}(S_4)_x(SO_4)_y$, in which the 0.22 mol of U were determined by ICP). Because in the starting material S_4-LDH, the total S moles are 0.52 (= 0.13 × 4), so we can list two equations of (1) $4x + y = 0.52$ and (2) $x + y = 0.22$, from which the values of $x = 0.10$ and $y = 0.12$ were calculated.

DOI: 10.1021/jacs.5b00762
J. Am. Chem. Soc. 2015, 137, 3670−3677

Scheme 1. Binding Modes of $[S_4]^{2-}$ with UO_2^{2+} and Arrangements of Gallery Species in LDH at Different Concentrations of UO_2^{2+} and Anions

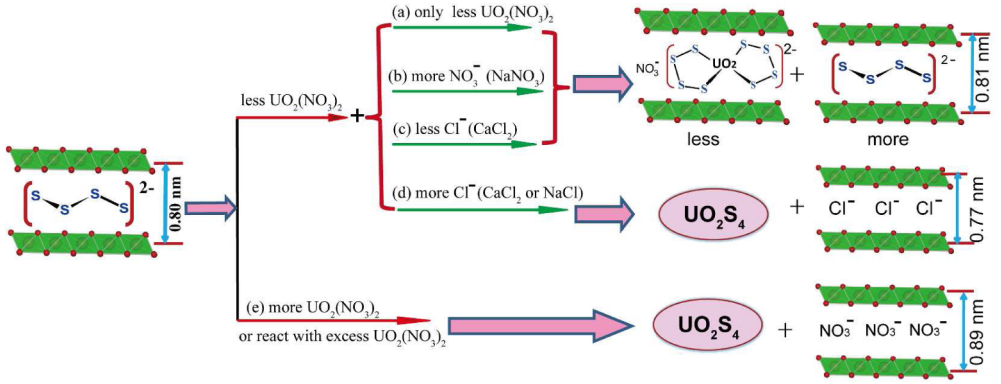

mined amount and the calculated values based on the as-obtained formula are in good agreement (see Table 7). These results are in a good agreement with the above analyses for uranium adsorption with S_4-LDH at various concentrations and confirm that at a high U concentration, the NO_3-LDH prefers to form, while other products such as UO_2S_4 and UO_2SO_4 are produced outside the LDH gallery (Scheme 1b). SEM images (see Figure 7c,c′) show that in addition to the dominated hexagonal prismatic plates for LDH,[47] many small U/S containing particles exist on the surface of the platelets (presumably UO_2S_4 and UO_2SO_4). The halo of the XRD pattern in the region of 20−50° (Figure 7a) indicates the presence of broad peaks associated with the two phases of UO_2S_4 and UO_2SO_4, in comparison with their patterns shown in Figure 7a′, 7a″.

Binding Modes of $(S_4)^{2-}$ with UO_2^{2+} and Guest Arrangements within LDH Gallery. Structural changes in the S_x-LDH samples after U adsorption are suggested by powder XRD as discussed above. Three d_{basal} of 0.81, 0.89, and 0.77 nm were observed depending on UO_2^{2+} concentrations or/and different anion types. Based on the above observations and the complexation chemistry of polysulfides, the mechanism of uranium capture is summarized as follows: (1) At low uranium concentration (1−120 ppm), where the S_4-LDH material is in large excess, the following reaction appears to lead to the uranium adsorption:

$$\text{LDH-}[(S_4)^{2-}]_x + yUO_2(NO_3)_2 \rightarrow \text{LDH-}[(S_4)^{2-}]_{x-2y} + \text{LDH-}\{[UO_2(S_4)_2]^{2-}\}_y(NO_3^-)_{2y} \quad (x \gg y) \qquad (1)$$

In this case, because the $(S_4)^{2-}$ anions are in large excess relative to UO_2^{2+}, two $(S_4)^{2-}$ may preferentially coordinate with one UO_2^{2+} to form $[UO_2(S_4)_2]^{2-}$ anionic complexes, which are retained in the LDH interlayer. Similar polysulfide complexes had been synthesized and structurally characterized in the literautre.[36] Because $x \gg y$, the dominant interlayer anions are are still $[S_4]^{2-}$, the resulting d_{basal} is at 0.81 nm (Scheme 1a). This reaction also seems to occur in the cases of "low U + high $NaNO_3$" (Scheme 1b) and "low U + less $CaCl_2$" (Scheme 1c). (2) In the case with low UO_2^{2+} concentration levels, if there exist anions such as Cl^- having high affinity for LDH layer, they will insert into the LDH gallery, and UO_2S_4 phase will be formed according Scheme 1d and eq 2:

$$\text{LDH-}[(S_4)^{2-}]_x + xUO_2(NO_3)_2 + 2xCl^- \rightarrow \text{LDH-}Cl_{2x} + x\,UO_2S_4 + 2xNO_3^- \quad (x \gg y) \qquad (2)$$

This occurs in the cases of "low U + high $CaCl_2$" and "low U + high NaCl" experiments. (3) When the UO_2^{2+} concentration levels are high, such as the adsorption at U > 120 ppm or reaction with excess $UO_2(NO_3)_2$, the U capture can be explained by Scheme 1e and eq 3:

$$\text{LDH-}[(S_4)^{2-}]_x + xUO_2(NO_3)_2 \rightarrow \text{LDH-}(NO_3^-)_{2x} + xUO_2S_4 \qquad (3)$$

CONCLUDING REMARKS

Based on the hypothesis that the uranium in the UO_2^{2+} is a relatively soft Lewis acid, we have demonstrated that the polysulfide/LDH materials, S_x-LDH, show a highly selective UO_2^{2+} removal in both aqueous solution and seawater due to the $UO_2^{2+}\cdots S^{2-}$ bonding interactions. The high K_d values (10^4−10^6 mg/L at 1−300 ppm), efficient removal capacities (q_m = 330 mg/g), and high % removal (>95% at 1−100 ppm) for UO_2^{2+} indicate the great potential of these materials for uranium capture and superiority over other reported adsorbents. The S_x-LDHs also show high selectivity for UO_2^{2+} against other hard cations such as Na^+ and Ca^{2+} even when their molar concentrations are 4 orders of magnitude higher. The S_x-LDH materials are effective for the removal of uranyl species from complex water and seawater samples containing trace levels of U (ppb) and are promising for uranium harvesting from the sea. In view of their environmentally benign constituents, S_x-LDHs are unique, potentially low-cost sorbents, for uranium sequestration from aqueous media relevant to nuclear waste.

AUTHOR INFORMATION

Corresponding Author

*m-kanatzidis@northwestern.edu

Notes

The authors declare no competing financial interest.

ACKNOWLEDGMENTS

This work is supported by the National Science Foundations of China (NSFC; nos. 21271028, 51272030, and 21271001) and the United States Department of Energy NEUP program.

DOI: 10.1021/jacs.5b00762
J. Am. Chem. Soc. 2015, 137, 3670−3677

REFERENCES

(1) Craft, E. S.; Abu-Qare, A. W.; Flaherty, M. M.; Garofolo, M. C.; Rincavage, H. L.; Abou-Donia, M. B. *J. Toxicol. Environ. Health, Part B* **2004**, *7*, 297.
(2) Gilman, A. P.; Villeneuve, D. C.; Secours, V. E.; Yagminas, A. P.; Tracy, B. L.; Quinn, J. M.; Valli, V. E.; Willes, R. J.; Moss, M. A. *Toxicol. Sci.* **1998**, *41*, 117.
(3) Favre-Reguillon, A.; Lebuzit, G.; Foos, J.; Guy, A.; Draye, M.; Lemaire, M. *Ind. Eng. Chem. Res.* **2003**, *42*, 5900.
(4) Schwochau, K. *Top Curr. Chem.* **1984**, *124*, 91.
(5) Onishi, H.; Sekine, K. *Talanta* **1972**, *19*, 473.
(6) Schmitt, P.; Beer, P. D.; Drew, M. G. B.; Sheen, P. D. *Tetrahedron Lett.* **1998**, *39*, 6383.
(7) Al-Attar, L.; Dyer, A. *J. Mater. Chem.* **2002**, *12*, 1381.
(8) Chiarizia, R.; Horwitz, E. P.; Alexandratos, S. D.; Gula, M. J. *Sep. Sci. Technol.* **1997**, *32*, 1.
(9) Fryxell, G. E.; Lin, Y. H.; Fiskum, S.; Birnbaum, J. C.; Wu, H.; Kemner, K.; Kelly, S. *Environ. Sci. Technol.* **2005**, *39*, 1324.
(10) Mellah, A.; Chegrouche, S.; Barkat, M. *J. Colloid Interface Sci.* **2006**, *296*, 434.
(11) Webb, S. M.; Fuller, C. C.; Tebo, B. M.; Bargar, J. R. *Environ. Sci. Technol.* **2006**, *40*, 771.
(12) Jang, J. H.; Dempsey, B. A.; Burgos, W. D. *Environ. Sci. Technol.* **2007**, *41*, 4305.
(13) Cantrell, K. J.; Kaplan, D. I.; Wietsma, T. W. *J. Hazard Mater.* **1995**, *42*, 201.
(14) Fiedor, J. N.; Bostick, W. D.; Jarabek, R. J.; Farrell, J. *Environ. Sci. Technol.* **1998**, *32*, 1466.
(15) Gu, B. H.; Wu, W. M.; Ginder-Vogel, M. A.; Yan, H.; Fields, M. W.; Zhou, J.; Fendorf, S.; Criddle, C. S.; Jardine, P. M. *Environ. Sci. Technol.* **2005**, *39*, 4841.
(16) Dushenkov, S.; Vasudev, D.; Kapulnik, Y.; Gleba, D.; Fleisher, D.; Ting, K. C.; Ensley, B. *Environ. Sci. Technol.* **1997**, *31*, 3468.
(17) Starvin, A. M.; Rao, T. P. *Talanta* **2004**, *63*, 225.
(18) Coleman, S. J.; Coronado, P. R.; Maxwell, R. S.; Reynolds, J. G. *Environ. Sci. Technol.* **2003**, *37*, 2286.
(19) Al-Hobaib, A. S.; Al-Suhybani, A. A. *J. Radioanal Nucl. Ch.* **2014**, *299*, 559.
(20) Ulusoy, H. I.; Simsek, S. *J. Hazard Mater.* **2013**, *254*, 397.
(21) Monier, M.; Elsayed, N. H. *J. Colloid Interface Sci.* **2014**, *423*, 113.
(22) Nakajima, A.; Sakaguchi, T. *J. Radioanal. Nucl. Chem.* **1994**, *178*, 319.
(23) Sakaguchi, T.; Nakajima, A. *Sep. Sci. Technol.* **1987**, *22*, 1609.
(24) Liao, X. P.; Lu, Z. B.; Du, X.; Liu, X.; Shi, B. *Environ. Sci. Technol.* **2004**, *38*, 324.
(25) Metilda, P.; Gladis, J. M.; Rao, T. P. *Radiochim. Acta* **2005**, *93*, 219.
(26) Liu, J.; Li, J.; Yang, X. D.; Song, Q.; Bai, C. Y.; Shi, Y.; Zhang, L.; Liu, C. X.; Li, S. J.; Ma, L. J. *Mater. Lett.* **2013**, *97*, 177.
(27) Li, B.; Ma, L. J.; Tian, Y.; Yang, X. D.; Li, J.; Bai, C. Y.; Yang, X. Y.; Zhang, S.; Li, S. J.; Jin, Y. D. *J. Hazard. Mater.* **2014**, *271*, 41.
(28) McKinley, J. P.; Zachara, J. M.; Smith, S. C.; Turner, G. D. *Clays Clay Miner.* **1995**, *43*, 586.
(29) Sharma, P.; Tomar, R. *Micropor. Mesopor. Mater.* **2008**, *116*, 641.
(30) Marinin, D. V.; Brown, G. N. *Waste Manage.* **2000**, *20*, 545.
(31) Wersin, P.; Hochella, M. F.; Persson, P.; Redden, G.; Leckie, J. O.; Harris, D. W. *Geochim. Cosmochim. Acta* **1994**, *58*, 2829.
(32) Descostes, M.; Schlegel, M. L.; Eglizaud, N.; Descamps, F.; Miserque, F.; Simoni, E. *Geochim. Cosmochim. Acta* **2010**, *74*, 1551.
(33) Borah, D.; Senapati, K. *Fuel* **2006**, *85*, 1929.
(34) Ozverdi, A.; Erdem, M. *J. Hazard Mater.* **2006**, *137*, 626.
(35) Sutorik, A. C.; Kanatzidis, M. G. *J. Am. Chem. Soc.* **1997**, *119*, 7901.
(36) Sutorik, A. C.; Kanatzidis, M. G. *Polyhedron* **1997**, *16*, 3921.
(37) Manos, M. J.; Kanatzidis, M. G. *J. Am. Chem. Soc.* **2012**, *134*, 16441.
(38) (a) Riley, B. J.; Chun, J.; Um, W.; Lepry, W. C.; Matyas, J.; Olszta, M. J.; Li, X. H.; Polychronopoulou, K.; Kanatzidis, M. G. *Environ. Sci. Technol.* **2013**, *47*, 7540. (b) Bag, S.; Arachchige, I. U.; Kanatzidis, M. G. *J. Mater. Chem.* **2008**, *18*, 3628−3632. (c) Bag, S.; Gaudette, A. F.; Bussell, M. E.; Kanatzidis, M. G. *Nature Chemistry* **2009**, *1*, 217−224. (d) Chalcogels: Bag, S.; Kanatzidis, M. G. *J. Am. Chem. Soc.* **2010**, *132*, 14951−14959. (e) Oh, Y.; Bag, S.; Malliakas, C. D.; Kanatzidis, M. G. *Chem. Mater.* **2011**, *23*, 2447−2456. (f) Shafaei-Fallah, M.; He, J.; Rothenberger, A.; Kanatzidis, M. G. *J. Am. Chem. Soc.* **2011**, *133*, 1200−1202. (g) Yuhas, B. D.; Prasittichai, C.; Hupp, J. T.; Kanatzidis, M. G. *J. Am. Chem. Soc.* **2011**, *133*, 15854−15857. (i) Yuhas, B. D.; Smeigh, A. L.; Samuel, A. P. S.; Shim, Y.; Bag, S.; Douvalis, A. P.; Wasielewski, M. R.; Kanatzidis, M. G. *J. Am. Chem. Soc.* **2011**, *2011*, 7252−7255.
(39) Khan, A. I.; O'Hare, D. *J. Mater. Chem.* **2002**, *12*, 3191.
(40) Constantino, V. R.; Pinnavaia, T. J. *Catal. Lett.* **1994**, *23*, 361.
(41) Corma, A.; Fornes, V.; Rey, F.; Cervilla, A.; Llopis, E.; Ribera, A. *J. Catal.* **1995**, *152*, 237.
(42) Gérardin, C.; Kostadinova, D.; Sanson, N.; Coq, B.; Tichit, D. *Chem. Mater.* **2005**, *17*, 6473.
(43) Ma, S. L.; Wang, J.; Du, L.; Fan, C. H.; Sun, Y. H.; Sun, G. B.; Yang, X. J. *Eur. J. Inorg. Chem.* **2013**, 1363.
(44) Rives, V.; Angeles Ulibarri, M. *Coord. Chem. Rev.* **1999**, *181*, 61.
(45) Xue, X. Y.; Gu, Q. Y.; Pan, G. H.; Liang, J.; Huang, G. L.; Sun, G. B.; Ma, S. L.; Yang, X. J. *Inorg. Chem.* **2014**, *53*, 1521.
(46) Ma, S. L.; Chen, Q. M.; Li, H.; Wang, P. L.; Islam, S. M.; Gu, Q. Y.; Yang, X. J.; Kanatzidis, M. G. *J. Mater. Chem. A* **2014**, *2*, 10280.
(47) Ma, S. L.; Shim, Y.; Islam, S. M.; Subrahmanyam, K. S.; Wang, P. L.; Li, H.; Wang, S. C.; Yang, X. J.; Kanatzidis, M. G. *Chem. Mater.* **2014**, *26*, 5004.
(48) Ma, S. L.; Islam, S. M.; Shim, Y.; Gu, Q. Y.; Wang, P. L.; Li, H.; Sun, G. B.; Yang, X. J.; Kanatzidis, M. G. *Chem. Mater.* **2014**, *26*, 7114.
(49) Oh, Y.; Morris, C. D.; Kanatzidis, M. G. *J. Am. Chem. Soc.* **2012**, *134*, 14604.
(50) Iyi, N.; Matsumoto, T.; Kaneko, Y.; Kitamura, K. *Chem. Mater.* **2004**, *16*, 2926.
(51) Ma, S. L.; Fan, C. H.; Du, L.; Huang, G. L.; Yang, X. J.; Tang, W. P.; Makita, Y.; Ooi, K. *Chem. Mater.* **2009**, *21*, 3602.
(52) Ma, S. L.; Wang, J.; Du, L.; Sun, Y. H.; Gu, Q. Y.; Sun, G. B.; Yang, X. J. *J. Colloid Interface Sci.* **2013**, *393*, 29.
(53) Ma, S. L.; Du, L.; Wang, J.; Chu, N. K.; Sun, Y. H.; Sun, G. B.; Yang, X. J.; Ooi, K. *Dalton Trans.* **2011**, *40*, 9835.
(54) Manos, M. J.; Ding, N.; Kanatzidis, M. G. *Proc. Natl. Acad. Sci. U.S.A.* **2008**, *105*, 3696.
(55) Lehto, J.; Clearfield, A. *J. Radioan. Nucl. Chem. Lett.* **1987**, *118*, 1.
(56) Liu, Z. P.; Ma, R. Z.; Osada, M.; Iyi, N.; Ebina, Y.; Takada, K.; Sasaki, T. *J. Am. Chem. Soc.* **2006**, *128*, 4872.
(57) Cavani, F.; Trifiro, F.; Vaccari, A. *Catal. Today* **1991**, *11*, 173.
(58) Froideval, A.; Del Nero, M.; Barillon, R.; Hommet, J.; Mignot, G. *J. Colloid Interface Sci.* **2003**, *266*, 221.
(59) Allen, G. C.; Crofts, J. A.; Curtis, M. T.; Tucker, P. M.; Chadwick, D.; Hampson, P. J. *J. Chem. Soc. Dalton* **1974**, 1296.
(60) Smart, R. S. C.; Skinner, W. M.; Gerson, A. R. *Surf. Interface Anal.* **1999**, *28*, 101.
(61) Islam, S. M.; Im, J.; Freeman, A. J.; Kanatzidis, M. G. *Inorg. Chem.* **2014**, *53*, 4698.
(62) Moulder, J. F.; Stickle, W. F.; Sohol, P. E.; Bomben, K. D. *Handbook of X-ray photoelectron spectroscopy*, Chastain, J., King, R. C., Jr., Ed.; Physical Electronics, Inc.: Eden Prairie, MN, 1995.
(63) Egawa, H.; Nonaka, T.; Abe, S.; Nakayama, M. *J. Appl. Polym. Sci.* **1992**, *45*, 837.
(64) Tabushi, I.; Kobuke, Y.; Nishiya, T. *Nature* **1979**, *280*, 665.
(65) Brancatelli, G.; Pappalardo, A.; Sfrazzetto, G. T.; Notti, A.; Geremia, S. *Inorg. Chim. Acta* **2013**, *396*, 25.
(66) Amayri, S.; Arnold, T.; Reich, T.; Foerstendorf, H.; Geipel, G.; Bernhard, G.; Massanek, A. *Environ. Sci. Technol.* **2004**, *38*, 6032.

DOI: 10.1021/jacs.5b00762
J. Am. Chem. Soc. 2015, 137, 3670−3677